Liquid Crystals
Publication details, including instructions for authors and subscription information:
http://www.informaworld.com/smpp/title~content=t713926090

Defect controlled dynamics of nematic liquids

Alejandro D. Rey[a]
[a] Department of Chemical Engineering, McGill University, Montreal, Canada

To cite this Article Rey, Alejandro D.(1990) 'Defect controlled dynamics of nematic liquids', Liquid Crystals, 7: 3, 315 — 334
To link to this Article: DOI: 10.1080/02678299008033809
URL: http://dx.doi.org/10.1080/02678299008033809

LIQUID CRYSTALS, 1990, VOL. 7, NO. 3, 315–334

Defect controlled dynamics of nematic liquids

by ALEJANDRO D. REY
Department of Chemical Engineering, McGill University, Montreal, Quebec H3A 2A7, Canada

(*Received 7 December 1989; accepted 6 October 1989*)

The long time dynamical response of a nematic liquid exhibiting banded textures (inversion walls) during the twist Freedericksz transition is presented. A dynamical model of approach to equilibrium through defect interaction and the resulting dissolution of the banded textures is presented. A linear stability analysis shows that splay-bend inversion wall defects are unstable to two dimensional infinitesimal perturbations. A model of inversion wall segment collapse with production of a disclination line pair is given. The energy-momentum tensor gives the force of interaction between inversion walls and disclination lines. A perturbation analysis gives the evolution of the director field in closed form. Entropy production gives the velocity of each line. The growth law governing the wall dissolution is given.

1. Introduction

Transient periodic textures are usually present in nematic polymers, lyotropic nematics, and some low molar mass nematics when subjected to orienting magnetic fields of sufficient strength. These periodic textures, also known as banded textures, are not stable and eventually disappear. The short time behaviour of band formation during magnetic reorientation has been extensively studied, experimentally [1–7], and theoretically [8–14], and is well understood. The long time behaviour of band disappearance has been less studied experimentally [1, 15], and there is no analysis, to the authors knowledge, of this phenomena.

The experimental evidence indicates that the periodic textures are transient and metastable, and that the true equilibrium state is, neglecting wall regions, a homogeneous texture. This paper presents a model of the long time response of nematic liquids exhibiting periodic textures during magnetic reorientation. The analysis explains how the metastable banded textures, formed at early times, evolve and eventually disappear, leaving behind a homogeneous texture. It will be shown that the mechanics of banded texture's disappearance are governed by defect interactions. We restrict the analysis to the geometrical arrangement that produces the twist Freedericksz transition [16, 17]. We expect the analysis to be applicable to nematic polymers, lyotropic nematics, and low molar mass nematics exhibiting periodic textures during magnetic reorientation.

Nematic liquids are diamagnetic and viscoelastic. The average molecular orientation is described by a unit vector **n**, whose direction is affected by the presence of electromagnetic fields, flow fields, and bounding surfaces. The liquid responds to the above orienting fields through its anisotropic magnetic susceptibility, anisotropic viscosities, and curvature elasticity. If a nematic liquid has a positive anisotropic magnetic susceptibility a sufficiently high magnetic field will tend to co-align the

0267-8292/90 $3.00

director everywhere except in a small region near the surfaces [16, 17]. A transient periodic response during magnetic reorientation gives rise to banded textures when the material is viewed under polarized light. This is a common phenomena in nematics when an oriented sample is subjected to a sufficiently strong field transverse to the initial uniform orientation. This periodic response is due to a coupling between fluid flow and director reorientation, in which opposed rotating regions produce shear flows characterized by lower viscosities than those in pure rotation.

Another characteristic nematic phenomena relevant to this work are the production and interaction of defects [16, 18]. Singular defects are described by strength and dimension. The strength of a defect quantifies the amount of distortion in the director field. In addition to singular lines and points defects, nematic liquids exhibit non-singular inversion wall defects. Singular and non-singular defects interact with each other and with the bounding surfaces. Inversion wall-disclination line interactions lead to the displacement of the disclination line in the direction of the inversion wall, while line–line interactions lead to their mutual attraction or repulsion according to whether their strengths have different or equal signs [16, 18] respectively.

Recently it has been shown that the banded textures are in fact splay–bend inversion walls [14]. These inversion walls contain continuous but large molecular orientation gradients within a small length and we can expect that they became unstable at large magnetic field intensities. In this work we show that instability of a splay–bend wall (band) to localized small wave length fluctuations results in the production of a disclination line pair of strength $\pm 1/2$ and in the collapse of a splay–bend inversion wall segment. Experimental evidence confirms the existence of this phenomena, known by the name of 'pincement' [1, 16, 19, 20]. The disclination line pair interacts with the surrounding splay–bend inversion wall and the resulting director field will evolve to minimize the magnetic and elastic free energy. The defect interaction (inversion wall-disclination line pair) controls the dynamics of the decay from the metastable state (banded texture) towards the true equilibrium state (homogeneous texture).

In this work we use the Leslie–Ericksen (L–E) theory of nematic continua [21, 22] to describe the temporal evolution of the macroscopic orientation field, the production and interaction of splay–bend inversion walls and line defects. In §2 we give a brief classification of defects that are solutions to the L–E equations. In §3 we briefly describe the twist Freedericksz transition and the formation of splay–bend inversion wall defects. We show that splay–bend walls are linearly unstable to two dimensional out-of-plane infinitesimal perturbations and result in a splay–bend inversion wall segment collapse with the production of a disclination line pair of strength $\pm 1/2$. In §4 we show, using the energy-momentum tensor, that a disclination line embedded in a splay–bend inversion wall is subjected to a pulling force equal to the surface tension of the inversion wall. A perturbation solution, valid for weak fields, gives the evolving director field in the proximity of the line. Entropy production is used to calculate the velocity of the line, and the time required for the wall dissolution. In §5 the analysis is extended to a disclination pair embedded in a splay–bend inversion wall. We present closed form expressions for the velocity of each line, and the forces acting on each line, and obtain the growth law governing the inversion wall disappearance. Finally, we discuss the results within the context of nucleation and growth phenomena, and present expressions for the nucleation rates, the critical droplet radius, and energy of activation.

2. Defect solutions to the Leslie–Ericksen equations

The free energy density of elastic deformation, W, is given in the L–E theory by

$$2W = K_{11}(\nabla \cdot \mathbf{n})^2 + K_{22}(\mathbf{n} \cdot \nabla \times \mathbf{n})^2 + K_{33} \| \mathbf{n} \times \nabla \times \mathbf{n} \|^2 \tag{1}$$

where K_{11}, K_{22}, and K_{33} are the elastic constants for splay, twist, and bend, respectively. The kinematic variables are the velocity, $\mathbf{v}$, and the director, $\mathbf{n}$. The momentum and director balance equations, in the absence of bulk flow and bulk external forces, reduce to

$$0 = t_{ji,j} \tag{2}$$

and

$$0 = G_i + g_i + \pi_{ji,j} \tag{3}$$

where $\mathbf{t}$ and π are the bulk and director stress tensors, respectively. $\mathbf{G}$ is the external director body force, and $\mathbf{g}$ is the intrinsic director body force. The constitutive equations, in the absence of bulk flow reduce to

$$t_{ji} = -p_0\delta_{ji} + t^e_{j,i} + \alpha_2\dot{n}_i + \alpha_3 n_i\dot{n}_j, \tag{4}$$

$$t^e_{ji} = W\delta_{ji} - \frac{\partial W}{\partial n_{k,j}} n_{k,i}, \tag{5}$$

$$g_i = \gamma n_i - \beta_j n_{i,j} - \frac{\partial W}{\partial n_i} - \lambda_1\dot{n}_i, \tag{6}$$

$$\pi_{ji} = \beta_j n_i - \frac{\partial W}{\partial n_{i,j}}, \tag{7}$$

where t^e_{kj} is the Ericksen stress tensor that introduces the elastic effects on the stress field, $\lambda_1 = \alpha_3 - \alpha_2$ is the rotational viscosity, and α_2 and α_3 are two Leslie viscosity coefficients. The scalar functions $-p_0 + W$, γ, and the vector function β arise because of the constraints of incompressibility and director unit length. The superposed dot on the director denotes its material derivative.

Inversion walls are steady one dimensional solutions to the L–E equations of nematics subjected to homogeneous magnetic fields, and also to converging flows [23]. The walls arise due to the degeneracy of reorientation when a nematic is subjected to an orienting field. Using cartesian (x, z) coordinates, the equation for the director $\mathbf{n}$ field, assuming that $n_x = \sin\theta$, $n_z = \cos\theta$, in the presence of a magnetic field $\mathbf{H} = (H, 0)$ is

$$K\frac{\partial^2\theta}{\partial z^2} + \chi_a H^2 \sin\theta\cos\theta = 0. \tag{8}$$

This equation with the following boundary conditions: $\theta(-\infty) = +(\pi/2)$; $\theta(+\infty) = -(\pi/2)$ admits an inversion wall solution [24] given by

$$\theta(z) = -2\tan^{-1}\exp\left[z\sqrt{\left(\frac{\chi_a H^2}{K}\right)}\right] + \frac{\pi}{2}, \tag{9}$$

where χ_a is the anisotropic magnetic susceptibility. As the director traverses the wall, it rotates by π radians within a spatial length d of the order $\sqrt{(K/\chi_a H^2)}$. Figure 1 give an schematic of three common walls, the splay–bend walls and the twist wall. Using the one constant approximation ($K = K_{11} = K_{22} = K_{33}$) equation (9) describes the

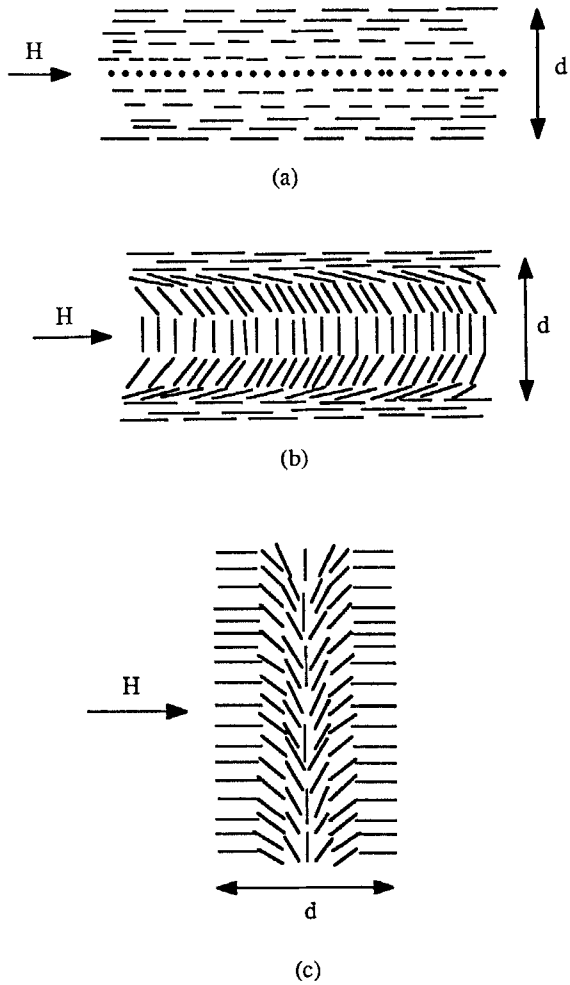

Figure 1. Schematic diagrams of inversion walls. (*a*) Twist wall. (*b*) Splay–bend wall parallel to H. (*c*) Splay–bend wall perpendicular to H. H is the magnetic field strength, and d is the wall thickness.

director field of the three walls. In addition to two dimensional non-singular defects, steady planar singular director fields are also solutions to the L–E equations. Again, using the one constant approximation, the governing Laplace equation [25]

$$\nabla^2\theta = 0 \tag{10}$$

admits singular solutions of the form

$$\theta = S\tan^{-1}\frac{z}{x} + U, \tag{11 a}$$

$$S = \pm\frac{m}{2}, \tag{11 b}$$

where S is the strength of the disclination, U is a constant, and m is a integer. The line is along the $-y$ direction and the director jumps by an integral multiple of π radians as a circuit is traversed around it. Figures 2 shows the director pattern in the

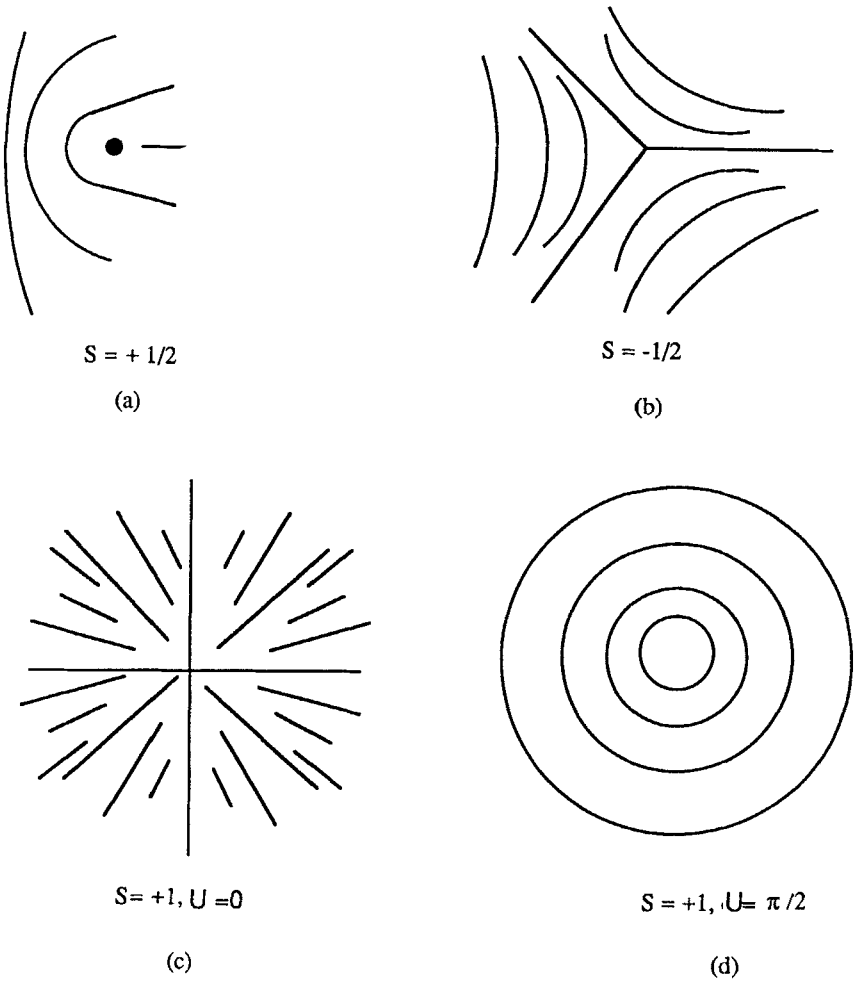

Figure 2. Director patterns in the proximity of common disclinations.

proximity of some common disclination lines. If the disclination line travels in the x-direction with a small constant velocity v, due to an elastic interaction, the director field

$$\theta = S\tan^{-1}\frac{z}{x - vt} + U, \tag{11 c}$$

where t is time, is a good [26] approximation to

$$K\nabla^2\theta = \lambda_1 \frac{\partial\theta}{\partial t} \tag{11 d}$$

In fact equation (11 c) is the first order term in a perturbation solution of equation (11 d). (Higher order terms can be obtained using the method shown in §4). In the presence of orienting magnetic fields and bounding surfaces, the dynamics of a planar director field, in the one constant approximation, satisfies

$$K\left[\frac{\partial^2\theta}{\partial x^2} + \frac{\partial^2\theta}{\partial z^2}\right] + \chi_a H^2 \sin\theta\cos\theta = \lambda_1 \frac{\partial\theta}{\partial t}. \tag{12}$$

The above equation is the balance of the elastic, magnetic, and rotational torques, respectively, acting on the director. Equations (8) and (10) are particular cases of equation (12) and their solutions are also particular solutions to equation (12). The inversion wall solution (equation (9)) is a steady state z-dependent solution of equation (12). The static disclination line solution (equation (11 a)) is a steady state solution of equation (12) for vanishing field strengths. The moving disclination line solution (equation (11 c)) is a first order approximation to equation (12) for vanishing field strengths. We shall obtain a solution of equation (12), valid for weak fields, that contains static inversion walls and moving disclination lines. We conclude that the L–E theory can model the evolution of a director field containing inversion walls and travelling disclination lines.

3. Splay–bend inversion wall stability in the twist Freedericksz transition of a nematic liquid

The periodic twist Freedericksz transition is best represented in cartesian coordinates (x, y, z). The initial state is one of uniform alignment in the z-direction with a director field $\mathbf{n}_0 = (0, 0, 1)$. At time $t = 0$ a uniform magnetic field is imposed in the x-direction $\mathbf{H} = (H, 0, 0)$. The x–z plane is assumed to be of infinite extent. If one assumes a director field of the form: $\mathbf{n} = (\sin\theta, 0, \cos\theta)$, where $\theta(y, z, t)$ describes the in-plane angle of the director relative to the initial orientation, and a velocity field $v = (u, 0, 0)$ then the steady state solutions to the full L–E equations are splay–bend inversion walls [14]. A transient optical microscopy simulation using the L–E equations describe the formation of the banded textures [14], in agreement with experiments [15].

As already stated the periodic response during the twist Freedericksz transition is due to the strong coupling between fluid flow and director reorientation, in which opposed rotating regions produce shear flows characterized by lower viscosities than those in pure rotation. This kinematic mechanism favors short wave lengths, but short wave lengths increase the elastic energy. The competing effects find an optimal balance, resulting in a fastest growing mode [3].

The lowest energy state is achieved by minimizing the elastic and magnetic energies. Neglecting the bounding surfaces, this obtains with a director field co-linear with the imposed magnetic field. But the system is driven to a high energy metastable state by the formation of splay–bend wall defects. To lower the elastic energy, the splay–bend inversion walls can evolve into lower energy twist walls. The twist inversion walls still contain large magnetic and elastic energy, and a collapse by the production of lines is expected. A more plausible scenario is that a series of wall segments can collapse by the production of disclination pairs, and subsequently the line pairs will interact with the rest of the inversion wall. The interaction leads to the displacement of the lines, and this displacement dissolves the inversion wall, leaving behind a homogeneous director field. This is analogous to nucleation and growth phenomena during the decay from a metastable state in a first order phase transition for a non-conserved order parameter system [27]. The system becomes unstable to small wavelength fluctuations and decays by the formation and growth of droplets (collapsed inversion wall segments) larger than a critical size.

We now turn to the linear stability analysis of splay–bend walls appearing during the twist Freedericksz transition, allowing for anisotropic elasticity. We assume a director $\theta(z)$ distribution describing a wall in the x-direction due to the presence of

a magnetic field $\mathbf{H} = (H, 0, 0)$ of sufficient strength, and impose in- and out-of-plane periodic two dimensional perturbations $\psi(x, z, t)$ and $\xi(x, z, t)$ respectively, resulting in a director field $\mathbf{n}(x, z, t)$ given by

$$n_x = \sin\theta + \psi\cos\theta, \tag{13a}$$

$$n_y = \xi, \tag{13b}$$

$$n_z = \cos\theta - \psi\sin\theta. \tag{13c}$$

Substituting this director field into equation (3), with the external director body force given by $G_i = \chi_a H_i H_j n_j$, retaining only linear terms, the evolution equation for the twist component $\xi(x, z, t)$ becomes

$$A(\theta)\xi + B(\theta)\xi_z + C(\theta)\xi_x + D(\theta)\xi_{zz} + E(\theta)\xi_{xx} + F(\theta)\xi_{xz} - \chi_a H^2\xi = \lambda_1\frac{\partial\xi}{\partial t}, \tag{14}$$

where the expressions for the coefficients A, B, C, D, E, and F are given in Appendix I. The boundary conditions are

$$\xi = 0 \quad \text{for all} \quad x, z \Rightarrow \pm\infty, \tag{15a}$$

$$\xi = 0 \quad \text{for} \quad x = 0, L \quad \text{and all } z. \tag{15b}$$

Equation (14) is parabolic with position dependent coefficients and must have solutions of the form

$$\xi = \exp(st) f(x, z). \tag{16}$$

It is convenient to scale the z-direction with the thickness of the splay–bend inversion wall $d = H^{-1}\sqrt{(K/\chi_a)}$, and the x-direction with the half wave-length L of the perturbation. In that case the evolution equation (14) becomes

$$L^2d^2[A - \chi_a H^2 - \lambda_1 s]f + L^2 dB\frac{\partial f}{\partial\tilde{z}} + Ld^2C\frac{\partial f}{\partial\tilde{x}} + L^2D\frac{\partial^2 f}{\partial\tilde{z}^2} + d^2E\frac{\partial^2 f}{\partial\tilde{x}^2} + LdF\frac{\partial^2 f}{\partial\tilde{x}\partial\tilde{z}} = 0 \tag{17}$$

where $\tilde{x} = x/L$, and $\tilde{z} = z/d$. This is an eigenvalue problem for the growth rate s. Steady solutions given by equation (9) will be unstable to out-of-plane two dimensional perturbations if any eigenvalue is positive. Marginal stability is defined by $s = 0$.

We use the linear approximation to the steady state wall profile to simplify the analysis

$$\theta(\tilde{z}) = \frac{\pi}{2}(1 - 2\tilde{z}), \tag{18}$$

in which case the boundary conditions given by equation (15*a*) are replaced by

$$\xi = 0 \quad \text{at} \quad \tilde{z} = 0, 1. \tag{19}$$

A spectral method [28] can be used to obtain approximate eigenfunctions. A double odd periodic expansion

$$f^a = \sum_{j=1}^{N}\sum_{k=1}^{N} a_{jk}\sin j\pi\tilde{x}\sin k\pi\tilde{z} \tag{20}$$

approximates f in an integral sense if the coefficient set a_{jk} satisfies

$$\int_0^1 \int_0^1 [R_{jk} \sin l\pi\tilde{x} \sin m\pi\tilde{z}] \, d\tilde{x}d\tilde{z} = 0, \tag{21}$$

where R_{jk}, the residual, is the left hand side of equation (17) with f^a replacing f. Equation (21) results in a matrix equation for the coefficient set

$$M_{lmjk} a_{jk} = 0 \tag{22}$$

The homogeneous matrix equation (22) has non-trivial solutions only if det (**M**) = 0. The sufficient condition for instability ($s \geqslant 0$) is obtained from this equation. For a one term ($N = 1$) double expansion the condition is

$$\pi^2(1 - K_{22}/K_{33}) \geqslant 1 + \frac{\pi^2}{4}(1 + 3K_{22}/K_{33}) \frac{d^2}{L^2}. \tag{23}$$

The ordering of the successive approximations establishes that the first eigenvalue is the most unstable [28]. In obtaining the threshold we have used the approximation $d^2 = K_{33}/\chi_a H^2$ instead of using an average of the splay and bend constants. This is a good approximation for most nematics [16, 17, 29].

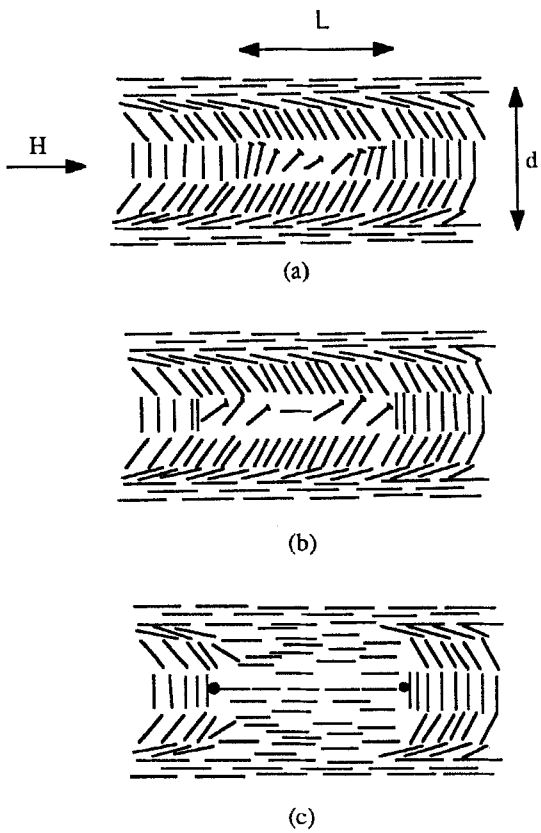

Figure 3. Schematic of a splay–bend wall dissolution. (*a*) The wall is unstable to two dimensional perturbations. (*b*) The non-linear evolution results in the nucleation of a $\pm 1/2$ disclination pair. (*c*) The wall pulls the lines apart, the velocity of the lines scales with the inverse of the wall thickness. L is the half wave length of the perturbation along the wall.

For sufficiently strong fields, the wall thickness may be small enough to make the inequality, given by equation (23), hold. The perturbation is periodic in the x-direction, and the length L is the segment of the wall that collapses by the appearance of an out-of-plane component. The out-of-plane component allows the director in the centre region of the collapsed wall to rotate in the direction of the applied field, thereby lowering the energy of the system. It is then plausible to assert that the non-linear resolution of the instability results in the collapse of a wall segment with a subsequent production of a disclination pair of strength $\pm 1/2$ as seen experimentally. Figures 3 (*a*), (*b*), (*c*) show a schematic of the evolution of the instability, the nucleation of a disclination pair, and the replacement of the wall by parallel alignment. A further discussion of the stability threshold for actual nematics will be given in §b, following the other essentials of the analysis.

4. Splay–bend wall-disclination line dynamics

The interruption of the wall by the presence of the disclination pair leads to the relative displacement of the line due to the pulling force exerted by the wall. If a line defect is moving, it is because of the pulling force due to a director field distortion enclosing the disclination. Therefore, to calculate the force we need to know the director pattern on a surface embracing the disclination. Once the director field and the force on the line are known, the velocity of the line follows from standard dissipative arguments. In this section we treat the interaction of a single disclination line embedded in a splay–bend inversion wall, and treat the wall-disclination pair interaction in the next one.

As shown by Eshelby [30], the integral of the energy-momentum tensor over a surface embracing a defect gives the Peach–Koehler force acting on it by the material outside the enclosing surface. For nematic continua the force is given by

$$F_k = \int_S \left[W\delta_{kj} - \frac{\partial W}{\partial n_{i,j}} n_{i,k} \right] dS_j \tag{24}$$

where S is a surface, or a circuit in two dimensions, enclosing the defect, and S_j is the component of the area vector in the direction of the normal unit vector $\boldsymbol{v}_j$. The expression between the brackets is the energy-momentum tensor. It turns out that the energy-momentum tensor is equal to the Ericksen stress tensor t^{e}_{kj}, given by equation (5), and therefore the force is real, and not a configurational fictitious force [30].

A schematic of a disclination line of strength $S = -1/2$ embedded in a splay–bend inversion wall is shown in figure 4 (*a*). We adopt a rectangular coordinate system fixed on the line. The magnetic and director fields are: $\mathbf{H} = (H, 0, 0)$ and $\mathbf{n} = (\sin\theta, 0, \cos\theta)$, respectively. The boundary conditions are

$$\theta(z) = -2\tan^{-1}\exp\left[z\sqrt{\left(\frac{\chi_a H^2}{K}\right)} \right] + \frac{\pi}{2} \quad \text{for} \quad x \Rightarrow +\infty, \tag{25}$$

$$\theta = -\frac{\pi}{2} \quad \text{for} \quad x \Rightarrow -\infty,\ z \geqslant 0, \tag{26}$$

$$\theta = -\frac{\pi}{2} \quad \text{for all} \quad x, z \Rightarrow +\infty, \tag{27}$$

$$\theta = +\frac{\pi}{2} \quad \text{for} \quad x \Rightarrow -\infty,\ z \leqslant 0, \tag{28}$$

$$\theta = +\frac{\pi}{2} \quad \text{for all} \quad x, z \Rightarrow -\infty. \tag{29}$$

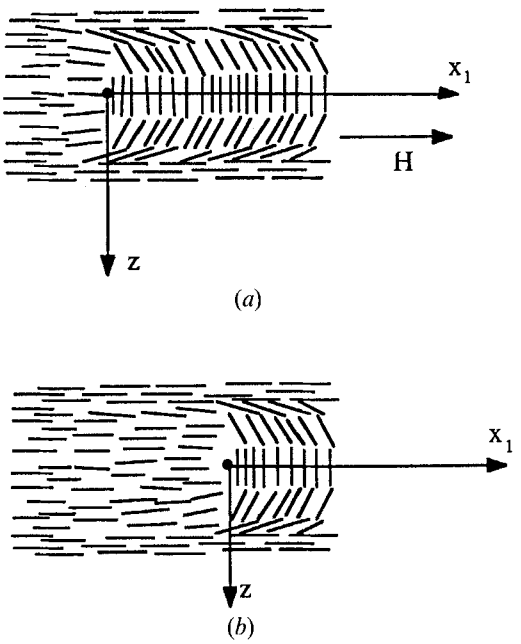

Figure 4. (*a*) Director field of a splay–bend inversion wall with a disclination line of strength $S = -1/2$ embedded in it. The coordinate system is fixed on the line. The magnetic field is in the x_1-direction. (*b*) The inversion wall pulls the line in the $+x_1$-direction. As the line travels, the inversion wall is replaced by parallel alignment.

We perform the integration using a suitable enclosing circuit along which the director field is known. Assuming that $K_{11} = K_{33}$ and that $n_x = \sin\theta$, $n_z = \cos\theta$, we integrate equation (24) around a square $L(a)$ enclosing the disclination cut and let its sides a go to infinity. Using the boundary conditions given by equations (25)–(29) we obtain $F_z = 0$ and

$$F_x = \int_{L(a)} t^e_{xj}\, dl_j = \lim_{a\to\infty} \int_{L(a)} t^e_{xj}\, dl_j = \int_{+\infty}^{-\infty} \left[\left(\frac{d\theta}{dz} \right)^2 - \frac{\chi_a H^2}{2} \sin^2\theta \right] dz = \frac{2K}{d}. \tag{30a}$$

The details are given in Appendix 2. The surface tension σ of the wall is the integral of the free energy density W across the wall,

$$\sigma = \int_{-\infty}^{+\infty} W\, dz \tag{30b}$$

whose value is precisely that given by equation (30*a*) if we define the wall thickness d by $d^2 = K/\chi_a H^2$, as calculated in [24]. We conclude that the wall surface tension or compressive force per unit length pulls, due to the wall sudden interruption, the disclination, causing it to move in the direction of the wall ($+x$-direction) with a constant velocity v that scales with the inverse of the wall thickness. The displacement of the disclination line replaces sharp orientation gradients (inversion wall) with homogeneous parallel alignment, as shown in figure 4(*b*).

To calculate the velocity of the disclination line we need the director field corresponding to a splay–bend wall-disclination line configuration. For generality we treat

a disclination of strength S. Since we look for a travelling disclination line solution, it is convenient to use a moving coordinate system fixed on the line

$$x_1 = x - vt, \tag{31a}$$

$$z = z. \tag{31b}$$

In this coordinate system equation (12) becomes

$$\nabla^2\theta + \frac{1}{d^2}\sin\theta\cos\theta = -\frac{\lambda_1 v}{K}\frac{\partial\theta}{\partial x_1}, \tag{32}$$

The boundary conditions are:

$$\theta = S\tan^{-1}\frac{z}{x_1} \quad \text{for} \quad x_1 \Rightarrow 0 \quad \text{and} \quad z \Rightarrow 0, \tag{33}$$

$$\theta(z) = -2\tan^{-1}\exp\left[z\sqrt{\left(\frac{\chi_a H^2}{K}\right)}\right] + \frac{\pi}{2} \quad \text{for} \quad x_1 \Rightarrow +\infty, \tag{34}$$

$$\theta = -\frac{\pi}{2} \quad \text{for} \quad x_1 \Rightarrow -\infty,\ z \geqslant 0, \tag{35}$$

$$\theta = -\frac{\pi}{2} \quad \text{for all} \quad x_1, z \Rightarrow +\infty, \tag{36}$$

$$\theta = +\frac{\pi}{2} \quad \text{for} \quad x_1 \Rightarrow -\infty,\ z \leqslant 0, \tag{37}$$

$$\theta = +\frac{\pi}{2} \quad \text{for all} \quad x_1, z \Rightarrow -\infty. \tag{38}$$

We seek weak field solutions ($d \Rightarrow \infty$) valid in the proximity of the disclination. Performing a parametric expansion in $1/d^2$, scaling lengths with $d(\tilde{x}_1 = x_1/d;\ \tilde{z} = z/d)$, and retaining the first order term, we obtain

$$\theta(\tilde{x}_1, \tilde{z}) \sim \theta_1 + \psi, \tag{39}$$

where θ_1 is the disclination line solution, and ψ is the perturbation due to the presence of the wall. Replacing equation (39) into the scaled equation (32) we obtain the set

$$\tilde{\nabla}^2\theta_1 = 0, \tag{40a}$$

$$\tilde{\nabla}^2\psi = -\frac{\lambda_1 v d}{K}\frac{\partial\theta_1}{\partial\tilde{x}_1}. \tag{40b}$$

The solution to equation (40a) is given by

$$\theta_1 = S\tan^{-1}\frac{\tilde{z}}{\tilde{x}_1}. \tag{41}$$

A separation of variables solution to equation (40b) of the form

$$\psi = R(\tilde{r})\sin\alpha, \tag{42}$$

where $(\tilde{r}, \alpha)$ are scaled polar coordinates ($\tilde{x} = \tilde{r}\cos\alpha$, $\tilde{z} = \tilde{r}\sin\alpha$), results in an ordinary differential equation for R

$$\frac{d^2R}{d\tilde{r}^2} + \frac{1}{\tilde{r}}\frac{dR}{d\tilde{r}} - \frac{R}{\tilde{r}^2} = \frac{\lambda_1 S\, dv}{K\tilde{r}}. \tag{43a}$$

Its general solution is

$$R = \frac{\lambda_1 Sdv}{2K} \tilde{r} \ln \tilde{r} + c_1 \tilde{r}. \tag{43b}$$

Finally, the perturbation ψ of the inversion wall on the line is given by

$$\psi = \frac{v\lambda_1 Sd}{2K} \tilde{z} \ln \tilde{r} + c_1 \tilde{z}. \tag{44}$$

To find the value of the constant c_1 we use the fact that the x-component of the Peach–Koehler force exerted by a director displacement ψ on the disclination is given by [30]

$$F_x = 2\pi SK \left[\frac{\partial \psi}{\partial z} \right]_{(0,0)}. \tag{45}$$

The force on the disclination is already given by equation (30a). To calculate the force according to equation (45) we calculate the limiting behavior of $(\partial\psi/\partial z)$ at the origin and get

$$F_x = \lim_{x,z \Rightarrow 0} 2\pi SK \frac{\partial \psi}{\partial z} = \frac{c_1 2\pi SK}{d}, \tag{46}$$

where we assumed that $v \Rightarrow 0$ as $d \Rightarrow \infty$ at least as fast as $\ln \tilde{r} \Rightarrow 0$ as $\tilde{r} = 0$. The validity of this assumption will be proven shortly. An explicit expression for c_1, valid for weak fields is obtained from equations (30a) and (46)

$$c_1 = \frac{1}{\pi S}.$$

The dynamics of the director field around the disclination line, in the weak magnetic field approximation, is given by

$$\theta \sim S \tan^{-1} \frac{\tilde{z}}{\tilde{x}_1} + \frac{v\lambda_1 Sd}{2K} \tilde{z} \ln \tilde{r} + \frac{1}{\pi S} \tilde{z}. \tag{47}$$

To obtain the velocity of the disclination line, caused by the pulling force exerted by the wall, we use the entropy balance equation [16, 31]

$$F_x v = T\dot{S}, \tag{48}$$

where $\dot{S}$ is the entropy production per unit length and per unit time, and is given in the L–E theory by

$$T\dot{S} = \int_{R^2} \lambda_1 \left(\frac{\partial \theta}{\partial t} \right)^2 d\mathbf{R}^2, \tag{49}$$

if back-flow effects are neglected and the director field is planar [32]. It follows from equation (40b) that

$$\frac{\partial \theta_1}{\partial t} = \frac{K}{\lambda_1} \nabla^2 \psi. \tag{50}$$

Replacing the right-hand side of equation (50) into equation (49) and performing the integration using polar coordinates, gives the entropy production to first order,

$$T\dot{S} = v^2 \lambda_1 S^2 \int_0^{2\pi} (\sin \alpha)^2 \, d\alpha \int_{r_c}^{d} r^{-1} \, dr = \pi v^2 \lambda_1 S^2 \ln \left(\frac{d}{r_c} \right), \tag{51}$$

where r_c is a molecular cut-off length introduced to avoid infinite energies [16, 18] and of the order of tens of Ångströms. The entropy production for a travelling disclination line embedded in a uniform director field is usually calculated using equation (11 *c*) and neglecting the velocity term [26, 31, 33]. The results agree with equation (51) except that a macroscopic distance replaces our inversion wall thickness. This consistency confirms the results (equation (47)) and the ordering of our perturbation analysis (equation (39)).

Finally, replacing the result of equation (51) and the value of the force F_x into equation (48) gives the expression for v as

$$v = \frac{2K}{\pi\lambda_1 dS^2 \ln(d/r_c)}. \tag{52}$$

As expected, the velocity scales with the inverse of the wall thickness, as the surface tension does. This scaling proves that the assumption used in obtaining equation (46) is correct. For vanishing field strengths not only does v vanishes but even the product vd vanishes as well. Lines involving stronger director distortions (larger S) will travel slower. Since v is a velocity describing convection of orientation it scales with the ratio of elastic to viscous effects (K/λ_1).

By replacing the value of v into equation (47) we obtain the director field in the proximity of the disclination line, as a function of the wall thickness d, the strength S of the disclination line defect, valid for weak fields,

$$\theta \sim S\tan^{-1}\frac{\tilde{z}}{\tilde{x}_1} + \frac{1}{\pi S \ln(d/r_c)}\tilde{z}\ln\tilde{r} + \frac{1}{\pi S}\tilde{z}. \tag{53}$$

The growth law of parallel alignment (homogeneous texture) is given by

$$t = \int_0^L \frac{dL}{v} = \frac{\lambda_1 \pi S^2 dL}{2K}\ln(d/r_c) \tag{54}$$

The growth law describes the phase transformation from banded textures to homogeneous textures. The spatial growth of the new phase is linear in time. It gives the time required to dissolve a length L of splay–bend inversion wall of thickness d by the dislacement of the disclination line of strength S. For typical values of nematic polymers: $\lambda_1 = 30$ poise, $K = 10^{-6}$ dynes, $r_c = 30$ Ångströms, $d = 5\,\mu$m, the displacement of the line will dissolve 0.08 cm of inversion wall per hour.

5. Splay–bend wall–disclination pair dynamics

In this section we analyze a disclination pair of strength $\pm 1/2$ embedded in the inversion wall, shown in figure 3 (*c*). In contrast to a single disclination line embedded in an inversion wall, there is no circuit enclosing one of the lines along which we know the director pattern *a priori*. That fact allowed us to calculate the constant c_1 and the main results of the previous section. We now assume that linear superposition is valid, although we note that the Ericksen stress tensor is non-linear. This is equivalent to assume that the director pattern between the disclinations is not affected by the presence of the surrounding wall. The magnitude of the force acting on each disclination line is

$$F_x = \left|\frac{2K}{d} - \frac{2K}{L}\pi S^2\right|, \tag{55}$$

where the second term on the right-hand side is the force of attraction between the disclination line pair of opposite signs separated by a distance L [16, 31]. We note that with this approximation the lines of strength $\pm 1/2$ get closer, separate, or remain at a constant distance whenever L is smaller, larger, or equal to $\pi d/4$, respectively. The existence of a critical distance for the dissolution of the banded textures is analogous to the existence of a critical droplet radius in the nucleation and growth of a new phase in a metastable phase during a first order phase transition.

We now follow the sequence of steps given in the previous section with minor changes. We seek a solution to equation (12) describing a slay–bend inversion wall with a disclination line pair of strength $\pm S$ embedded in it. We fix the coordinate system on one of the lines, say line 1 of strength $+S$. Again, the magnetic and director fields are $\mathbf{H} = (H, 0, 0)$ and $\mathbf{n} = (\sin\theta, 0, \cos\theta)$, respectively. The boundary conditions are given by Equations (34–38) and

$$\theta = S\tan^{-1}\frac{z}{x_1} - S\tan^{-1}\frac{z}{x_1 + L} \quad \text{for} \quad x_1 \Rightarrow 0 \quad \text{and} \quad z \Rightarrow 0.$$

As before we use $\pm S$ for the strengths of the lines, but note that walls collapse with production of $\pm 1/2$ disclination lines [20, 33]. We seek weak field solutions valid in the proximity of line 1 (The same analysis applies to line 2). Performing a parametric expansion in $1/d^2$, scaling lengths with d ($\tilde{x}_1 = x_1/d$; $\tilde{z} = z/d$), and retaining the first order term, we obtain

$$\theta(\tilde{x}_1, \tilde{z}) \sim \theta_1^1 + \psi^1, \tag{56}$$

where θ_1^1 is the disclination line pair solution, and ψ^1 is the perturbation due to the presence of the wall on line 1. The equations for θ_1^1 and ψ^1 are (40 *a*) and (40 *b*) respectively. The solution to equation (40 *a*) describing a line pair, separated by a distance L, in a frame fixed at the line of strength $+S$ is

$$\theta_1^1 = S\tan^{-1}\frac{\tilde{z}}{\tilde{x}_1} - S\tan^{-1}\frac{\tilde{z}}{\tilde{x}_1 + \tilde{L}}, \tag{57 a}$$

where $\tilde{L} = L/d$ is the scaled distance between the lines. The perturbation due to the splay–bend wall in the proximity of line 1 is

$$\psi^1 = \frac{v\lambda_1 Sd}{2K}\tilde{z}\ln\tilde{r} + \left(\frac{1}{\pi S} - \frac{d}{L}S\right)\tilde{z}, \tag{57 b}$$

where we have used the equality between equations (46) (evaluated using equation (57 *b*) and equation (55) to calculate the corresponding c_1 constant, as we did in the previous section). The dynamics of the director field in the proximity of line 1, in the weak field approximation, is

$$\theta \sim S\tan^{-1}\frac{\tilde{z}}{\tilde{x}_1} - S\tan^{-1}\frac{\tilde{z}}{\tilde{x}_1 + \tilde{L}} + \frac{v\lambda_1 Sd}{2K}\tilde{z}\ln\tilde{r} + \left[\frac{1}{\pi S} - \frac{dS}{L}\right]\tilde{z}. \tag{58}$$

To calculate the velocity of the lines we use the entropy balance equation (49). Following the same procedure as in the previous section, we obtain the entropy production due to the moving disclination line, to first order, as

$$T\dot{S} = \pi\lambda_1 v^2 S^2 \ln(L/r_c), \tag{59}$$

where the area of integration is a circular region of inner radius r_c and outer radius $L - r_c$. Again, it is instructive to compare previous calculations of the entropy

production for the case of a disclination line pair whose separation is changing in time, and is embedded in a homogeneous director field [26]. That calculation uses the dissipation due to the line pair and neglects the velocity terms in equation (57 *a*). It nevertheless agrees with our result (equation (59)) except for a numerical factor (1·213) multiplying L in the logarithmic term, arising from the fact that it is based in the dissipation of the disclination pair solution, and our calculation is based the dissipation of each line, using the perturbation of the wall on the line. Again, this consistency validates our results (equation (58) and our ordering (equation (56)). Using equation (48, 55, 59) we obtain the velocity of the travelling disclination line, embedded in a director field containing another disclination line and a splay–bend inversion wall,

$$v = \frac{2K\,[(1/\pi S) - (d/L)S]}{\lambda_1 dS \ln(Lr_c)}. \tag{60}$$

For very large separations we retrieve the wall-single line equation (the upper limit of the integral in equation (59) is changed from L to d). At the critical line separation $L_c = \pi d S^2$, the velocity vanishes. For line separations larger (smaller) than the critical one the distance increases (diminishes) with time.

The director field in the proximity of line 1, as a function of wall thickness d, line separation L, and defect strengths $\pm S$ is, in the weak magnetic field approximation

$$\theta^1 \sim S\tan^{-1}\frac{\tilde{z}}{\tilde{x}_1} - S\tan^{-1}\frac{\tilde{z}}{\tilde{x}_1 + \tilde{L}} + \frac{[(1/\pi S) - (d/L)S]}{\ln(L/r_c)}\,\tilde{z}\ln\tilde{r} + \left(\frac{1}{\pi S} - \frac{d}{L}S\right)\tilde{z}. \tag{61}$$

As expected, for $L \gg d$ we retrieve the wall-single line solution and each line behaves as in the previous section.

If the initial line separation is larger than the critical L_c, then the homogeneous textures will replace the banded textures. The growth law governing the kinetics of the transformation is

$$\int_{L_0}^{L} \frac{dL}{2v(L)} = \int_0^t dt \tag{62}$$

where L_0 is the initial line separation. Integrating, we obtain

$$\begin{aligned} t = {} & \frac{\lambda_1 dS^2\pi}{4K}\left\{\ln\left[\left[\frac{L}{r_c}\right]^{L}\left[\frac{r_c}{L_0}\right]^{L_0}\right] + [L_0 - L]\right\} \\ & + \frac{\lambda_1 dS^2\pi}{4K}\left\{\frac{\eta}{2}\left[\ln\frac{L-\eta}{L_0-\eta}\right]^2 + \eta^2\left[\frac{1}{L-\eta} - \frac{1}{L_0-\eta}\right]\right\} + \ldots, \end{aligned} \tag{63}$$

where $\eta = \pi S^2 d$. The growth law describes the phase transformation from banded textures to homogeneous textures. It gives the time required to dissolve a length L of splay–bend inversion wall of thickness d by the displacement of the disclination line pair of strength $\pm S$. The first term in the series gives the asymptotic late stage growth law, valid at long times.

6. Discussion

The banded textures are metastable and the system will not remain in this state but eventually will reach the true equilibrium state. If an initially aligned nematic liquid

is subjected to a magnetic field orthogonal to the initial orientation, the system develops a set splay–bend inversion walls separated by aligned regions. The nematic liquid will not remain in this state because there is a lower energy state consisting of coalignment of the director with the magnetic field (if $\chi_a > 0$). To reach this lower energy state the system nucleates inversion wall-free regions by the production of a disclination line pair. The analogous concept of a drop in the nucleation and growth of a new phase in a metastable phase is the collapsed wall bounded by the disclination pair. The surface tension of the drop is the line–line interaction in our case.

In §2 we showed that the walls are unstable to two dimensional perturbations. When the critical threshold given by equation (23) is exceeded, small segments of wall will collapse with the production of an array of disclination line pairs of strength $\pm 1/2$. We can assume that the collapsed wall segments are far apart such that we can neglect their interaction. According to equilibrium nucleation theory the number of droplets of size L is

$$n_L = N \exp -E_L/kT \tag{64}$$

where E_L is the free energy of formation of a droplet of size L, k is the Boltzmann constant, and T the temperature. N is a normalization constant. There are bulk and surface contributions to E_L. The bulk term E_b is the energy required to eliminate a wall of length L, that is, the energy required to rotate the director so that a parallel alignment is obtained,

$$E_b = -\sigma L d, \tag{65}$$

where σ is the surface tension of the wall given by equation (30 b). The surface term E_s is the energy required to nucleate a disclination line pair [16]

$$E_s = 2\pi S^2 K \ln \frac{L}{r_c} d. \tag{66}$$

The free energy of formation of a collapsed wall segment with the production of a disclination line pair is

$$E_L = -\sigma L d + 2\pi S^2 K \ln \frac{L}{r_c} d. \tag{67}$$

There is a competition between the energy required to collapse the wall (bulk term) and the energy of the disclination line pair (surface term). The disclination energy dominates at small L while the bulk term dominates at large L. As a consequence there is a critical distance Lc obtained from the condition $(dE_L/dL) = 0$,

$$L_c = \frac{2\pi S^2 K}{\sigma} = \pi S^2 d. \tag{68}$$

Collapsed wall segments of lengths larger than L_c will grow since they are energetically favored. These collapsed wall segments provide the mechanism of decay from the metastable state. The effect of increasing the magnetic field strength is to decrease the critical length. The rate of production I of collapsed wall segments, larger than the critical size, in a non-equilibrium steady-state is [27]

$$I = I_0 \exp -E_{L_c}/kT \tag{69}$$

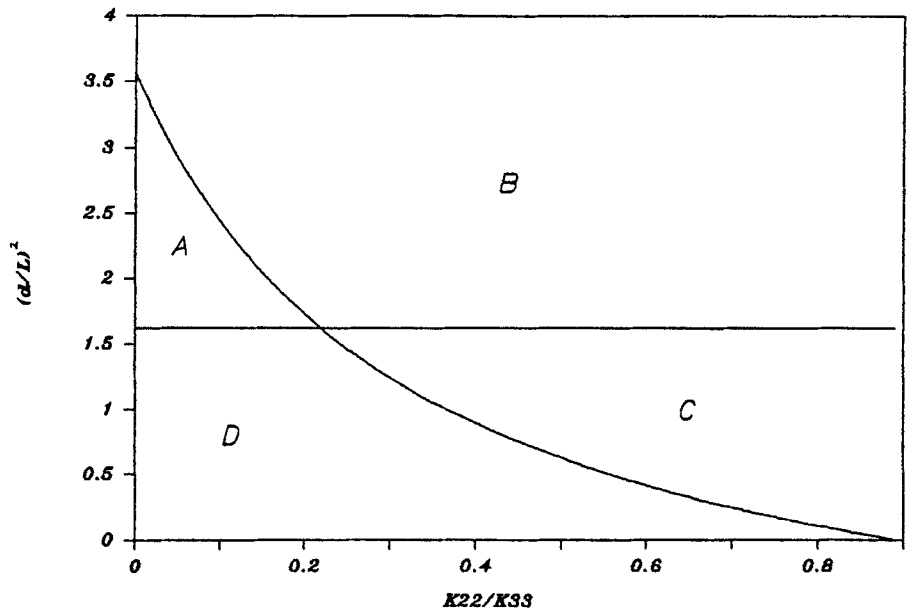

Figure 5. Inversion wall-parallel alignment transformation diagram. The horizontal line corresponds to the critical line separation L_c. The curve is the inversion wall stability threshold (equation (23)). *A*, walls are unstable, collapsed wall segments shrink; *B*, walls are stable; *C*, walls are stable; *D*, walls are unstable, collapsed wall segments grow.

where I_0 is the nucleation rate prefactor. This describes a thermally activated process, in which the energy of activation is the energy of formation of a critical collapsed wall segment

$$E_{L_c} = 2\pi S^2 K \left[\ln\left(\frac{\pi S d}{r_c} \right) - 1 \right] d. \tag{70}$$

A banded-homogeneous texture transformation diagram is shown in figure 5. It is obtained by plotting equations (23) and (68). These are four areas in the diagram: two above the horizontal line (*A*, *B*) showing the shrinkage of collapsed wall segments of length $L < L_c$, and two below (*C*, *D*) the horizontal line showing the growth of collapsed wall segments of length $L > L_c$. Even if the wall is unstable in area *A*, the initial line separation is not large enough to transform a wall into parallel alignment. In area *B* and *C* there is not enough elastic anisotropy for a wall collapse. Area *D* spans the magnitudes of L, d, and K_{22}/K_{33} for which a wall segment, unstable to two dimensional perturbations, will grow after its collapse. For actual nematics the elastic anisotropy required for wall instability is normally met. For example, for PLG (a nematic polymer) $K_{22}/K_{33} = 0.07$ [29], while for MBBA (a low molar mass nematic) $K_{22}/K_{33} = 0{\cdot}454$ [34]. The smaller the elastic anisotropy, the larger the critical length L_c, the higher the energy of activation E_c and the smaller the nucleation rate.

The main result of this work is growth law for homogeneous alignment given by equation (63). It can be used to estimate the time required to consume a length of inversion wall by the growth of a number n_L of collapsed wall segments of length $L > L_c$. If we have n_L droplets of average size L, the length L_w of wall consumed in

time t is

$$L_w = n_L L, \tag{71}$$

where L is given by equation (63). Better estimates require the time dependent size distribution function. Eventually we expect that the growing collapsed wall segments will interact with each other. Since the line pairs are embedded with alternate ordering in strength ($+-$ or $-+$) the approaching lines, separated by pulling wall segments, have different signs and will attract and annihilate each other. The final equilibrium state is a homogeneous texture with few or no disclination lines left.

In conclusion, the L–E theory of nematic continua is able to account for the collapse of inversion walls into pairs of disclination lines as seen experimentally. The effect of the surface tension of the wall is to pull the lines apart, thereby replacing a highly distorted director field for a homogeneous parallel alignment. The L–E theory is able to describe the kinetics of the metastable stage during the approach to equilibrium of important dynamical liquid crystal phenomena.

This work is supported by a grant from Fonds pour la Formation de Chercheurs et l'Aide á la Recherche of Québec, Canada.

Appendix I

The coefficients of the evolution equation (14) are

$$A(\theta) = [3(K_{33} - K_{22})\cos^2\theta + K_{22}]\theta_z^2 + [-K_{33}\cot\theta + (K_{33} - K_{22})\sin\theta\cos\theta]\theta_{zz}, \tag{A 1}$$

$$B(\theta) = [(K_{22} - K_{33})\sin 2\theta]\theta_z, \tag{A 2}$$

$$C(\theta) = [(K_{33} - K_{22})\cos 2\theta]\theta_z, \tag{A 3}$$

$$D(\theta) = (K_{33} - K_{22})\cos^2\theta + K_{22}, \tag{A 4}$$

$$E(\theta) = (K_{22} - K_{33})\cos^2\theta + K_{33}, \tag{A 5}$$

$$F(\theta) = (K_{33} - K_{22})\sin 2\theta. \tag{A 6}$$

Appendix II

To evaluate the integral in equation (24), we choose a square circuit $L(a)$ enclosing the line defect and let the sides a of the square increase to infinity. The circuit is traversed counter-clockwise, and the outward unit normals are the unit vectors in the $\pm x$ and $\pm z$ directions ($\pm\mathbf{i}$, $\pm\mathbf{k}$). The boundary conditions given by equations (25)–(29) indicate that the second term in the Ericksen stress tensor (equation (5)) makes no contribution along the chosen circuit. The z component is

$$F_z = \int_{L(a)} t^e_{zj}\,dl_j = \lim_{a\to\infty}\int_{L(a)} t^e_{zj}\,dl_j = -\int_{+\infty}^{-\infty} W(x, z = -\infty)\,dx + \int_{-\infty}^{+\infty} W(x, z = +\infty)\,dx = 0. \tag{A 7}$$

The x-component is

$$\left.\begin{aligned} F_x &= \int_{L(a)} t^e_{xj}\,dl_j = \lim_{a\to\infty}\int_{L(a)} t^e_{xj}\,dl_j = \int_{+\infty}^{-\infty} W(x = +\infty, z)\,dz, \\ F_x &= \int_{+\infty}^{-\infty} W(x = +\infty, z)\,dz. \end{aligned}\right\} \tag{A 8}$$

The total free energy density is [16]

$$W = \tfrac{1}{2}[K_{11}(\nabla \cdot \mathbf{n})^2 + K_{22}(\mathbf{n} \cdot \nabla \times \mathbf{n})^2 + K_{33} \| \mathbf{n} \times \nabla \times \mathbf{n} \|^2] - \tfrac{1}{2}\chi_a(\mathbf{n} \cdot \mathbf{H})^2 + \theta \text{ independent term.} \quad \text{(A 9)}$$

Replacing the given director and magnetic fields $\mathbf{H} = (H, 0, 0)$ and $\mathbf{n} = (\sin\theta, 0, \cos\theta)$ gives

$$W(x = +\infty, z) = \frac{K}{2}\left(\frac{d\theta}{dz}\right)^2 - \frac{\chi_a H^2}{2}\sin^2\theta + \theta \text{ independent term.} \quad \text{(A 10)}$$

The inversion wall satisfies equation (8) whose first integral is

$$K\left[\frac{\partial\theta}{\partial z}\right]^2 = \chi_a H^2 (\cos\theta)^2. \quad \text{(A 11)}$$

Using this equality the free energy density becomes

$$W(x = +\infty, z) = K\left(\frac{d\theta}{dz}\right)^2 + \theta \text{ independent term.} \quad \text{(A 12)}$$

Replacing this value into equation (A.8) gives

$$F_x = \int_{+\infty}^{-\infty} K\left(\frac{\partial\theta}{\partial z}\right)^2 dz = \int_{-\pi/2}^{+\pi/2} K\left|\frac{\partial\theta}{\partial z}\right| d\theta = 2H\sqrt{(K\chi_a)} = \frac{2K}{d}, \quad \text{(A 13)}$$

where we used

$$d = \frac{1}{H}\sqrt{\left(\frac{K}{\chi_a}\right)}.$$

References

[1] Fraden, S., Hurd, A. J., Meyer, R. B., Cahoon, M., and Caspar, D. L. D., 1985, *J. Phys., Paris*, **46**, C3-85.
[2] Lonberg, F., Fraden, S., Hurd, A. J., and Meyer, R. B., 1984, *Phys. Rev. Lett.*, **21**, 1903.
[3] Lonberg, F., and Meyer, R. B., 1985, *Phys. Rev. Lett.*, **55**, 718.
[4] Fincher, C. R., 1986, *Macromolecules*, **19**, 2431.
[5] Charvolin, J., and Hendrix, Y., 1986, *J. Phys. Lett., Paris*, **41**, L-597.
[6] Hui, Y. W., Kuzma, M. R., San Miguel, M., and Labes, M. M., 1985, *J. chem. Phys.*, **83**, 288.
[7] Kuzma, M. R., 1986, *Phys. Rev. Lett.*, **57**, 349.
[8] Hurd, A. J., Fraden, S., Lonberg, F., and Meyer, R. B., 1985, *J. Phys., Paris*, **46**, 905.
[9] Guyon, E., Meyer, R. B., and Salan, J., 1979, *Molec. Crystals liq. Crystals*, **54**, 261.
[10] Kini, U. D., 1988, *J. Phys., Paris*, **49**, 527.
[11] Miraldi, E., Oldano, C., and Strigazzi, A., 1986, *Phys. Rev.* A, **34**, 4348.
[12] Zimmermann, W., and Kramer, L., 1986, *Phys. Rev. Lett.*, **56**, 24.
[13] Sagues, F., and San Miguel, M., 1986, *Phys. Rev.* A, **33**, 2769.
[14] Rey, A. D., and Denn, M. M., *Liq. Crystals* (in the press).
[15] McClymer, J. P., and Labes, M. M., 1987, *Molec. Crystals liq. Crystals*, **144**, 275.
[16] de Gennes, P. G., 1974, *The Physics of Liquid Crystals* (Clarendon Press).
[17] Chandrasekhar, S., 1977, *Liquid Crystals* (Cambridge University).
[18] Kleman, M., 1983, *Points, Lines and Walls* (Wiley).
[19] Stieb, A., Baur, G., and Meier, G., 1975, *J. Phys., Paris*, **36**, C1-185.
[20] Meyer, R. B., 1973, *Molecular Fluids* (Proc. Les Houches Summer School).
[21] Ericksen, J. L., 1961, *Trans. Soc. Rheol.*, **5**, 23.
[22] Leslie, F. M., 1968, *Archs ration. Mech. Anal.*, **28**, 265.
[23] Rey, A. D., and Denn, M. M., 1989, *Liq. Crystals*, **4**, 253.
[24] Helfrich, W., 1968, *Phys. Rev. Lett.*, **21**, 1519.

[25] FRANK, F. C., 1958, *Discuss. Faraday Soc.*, **25**, 19.
[26] RANGANATH, G. S., 1983, *Molec. Crystals liq. Crystals*, **97**, 77.
[27] GUNTON, J. D., and DROZ, M., 1983, *Introduction to the Theory of Metastable and Unstable States* (Lectures Notes in Physics, Vol. 183) (Springer-Verlag).
[28] DENN, M. M., 1975, *Stability of Reaction and Transport Processes* (Prentice Hall).
[29] TARATUTA, V., HURD, A., and MEYER, R., 1985, *Phys. Rev. Lett.*, **55**, 246.
[30] ESHELBY, J. D., 1980, *Phil. Mag.* A, **42**, 403.
[31] IMURA, H., and OKANO, K., 1973, *Phys. Lett.* A, **42**, 403.
[32] CLADIS, P. E., and VAN SAARLOOS, W., 1988, *Solitons in Liquid Crystals*, edited by L. Lam and J. Prost (Springer-Verlag).
[33] DE GENNES, P. G., 1973, *Molecular Fluids* (Proc. Les Houches Summer School).
[34] HALLER, I., 1972, *J. chem. Phys.*, **51**, 1400.